Atmospheric Environment 252 (2021) 118295

Contents lists available at ScienceDirect

Atmospheric Environment

journal homepage: http://www.elsevier.com/locate/atmosenv

Ambient naphthalene and methylnaphthalenes observed at an urban site in the Pearl River Delta region: Sources and contributions to secondary organic aerosol

Hua Fang [a,c], Shilu Luo [a,c], Xiaoqing Huang [a,c], Xuewei Fu [a,c], Shaoxuan Xiao [a,c], Jianqiang Zeng [a,c], Jun Wang [a,c], Yanli Zhang [a,b,c], Xinming Wang [a,b,c,*]

[a] State Key Laboratory of Organic Geochemistry and Guangdong Key Laboratory of Environmental Protection and Resources Utilization, Guangzhou Institute of Geochemistry, Chinese Academy of Sciences, Guangzhou, 510640, China
[b] Center for Excellence in Urban Atmospheric Environment, Institute of Urban Environment, Chinese Academy of Sciences, Xiamen, 361021, China
[c] University of Chinese Academy of Sciences, Beijing, 100049, China

HIGHLIGHTS

- Ambient Nap and MN were measured at an urban site in the Pearl River Delta region.
- Total initial concentrations of Nap and MN were <2% of single-ring aromatics but contributed 12.4% of estimated SOA.
- The PMF model revealed vehicle exhaust as the largest source (~ 65%) of ambient Nap and MN.
- Biomass/coal burning emissions could account for ~30% of ambient Nap and MN.

GRAPHICAL ABSTRACT

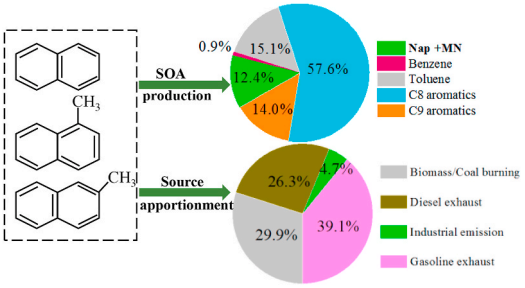

ARTICLE INFO

Keywords:
Naphthalene
Methylnaphthalenes
Intermediate-volatility organic compounds (IVOCs)
Photochemical ageing
Secondary organic aerosol (SOA)
Source apportionment

ABSTRACT

Naphthalene (Nap) and methylnaphthalenes (MN) are among important intermediate volatility organic compounds (IVOCs) that contribute substantially to the formation of secondary organic aerosols (SOA), yet studies about their ambient levels, source contributions and SOA productions are quite limited. In this study a field campaign was conducted from September 23rd to October 4th, 2019 at an urban site in the megacity Guangzhou in south China for characterizing ambient Nap and MN. Measured Nap, 2-MN, and 1-MN concentrations were 94.0 ± 23.1, 25.3 ± 4.5, and 11.8 ± 2.1 ng m^{-3} (mean ± 95% C.I.), respectively. Initial levels and chemical losses of Nap and MN were estimated using a photochemical age-based parameterization method, and results demonstrated that on average ~60% of Nap + MN were degraded during photochemical ageing. During the photochemically active period (12:00–15:00), Nap and MN could contribute 12.4% of estimated SOA formed from single-ring aromatics, Nap and MN altogether, while their initial levels were less than 2% of single-ring aromatics. Source apportioning by the positive matrix factorization (PMF) coupled with the photochemical age-based parameterization revealed that gasoline exhaust was the largest source, accounting for 39.1% of Nap and MN, followed by biomass/coal burning (29.9%), diesel exhaust (26.3%) and industrial emission (4.7%).

* Corresponding author. State Key Laboratory of Organic Geochemistry, Guangzhou Institute of Geochemistry, Chinese Academy of Sciences, 511 Kehua Rd, Tianhe, Guangzhou, 510640, China.
E-mail address: wangxm@gig.ac.cn (X. Wang).

https://doi.org/10.1016/j.atmosenv.2021.118295
Received 20 October 2020; Received in revised form 20 January 2021; Accepted 20 February 2021
Available online 26 February 2021

1. Introduction

Naphthalene (Nap) and methylnaphthalenes (1-methylnaphthalene and 2-methylnaphthalene, MN) are 2-ring aromatic hydrocarbons and a class of intermediate-volatility organic compounds (IVOCs), which recently have been revealed to be important secondary organic aerosol (SOA) precursors (Chan et al., 2009; Liu et al., 2015; Chen et al., 2016; Huang et al., 2019). However, these species were generally ignored in atmospheric models and emission inventories (Zhao et al., 2014). Based on previous chamber studies, the SOA production from Nap and MN was comparable to that from single-ring aromatics during the oxidation of gasoline exhaust and diesel exhaust, while Nap and MN could produce ~3.2 times more SOA than single-ring aromatics during oxidation of wood burning plumes (Chan et al., 2009; Liu et al., 2015). Besides, Nap and MN are also toxic air pollutants and could cause a number of adverse health effects (ATSDR, 2005; Loh et al., 2007; Lin et al., 2009; Dey et al., 2021). Their oxidation products in presence of OH radicals and NOx in ambient air, like nitronaphthalenes, methylnitronaphthalene and dicarbonyl derivates, might be even more mutagenic and carcinogenic than Nap and MN (Lundstedt et al., 2007; Wu et al., 2020).

The ambient Nap and MN with two aromatic rings are less volatile than single-ring aromatics, yet they exist largely in gas phase and are the most volatile and abundant species among airborne polycyclic aromatic hydrocarbons (PAHs) (Lu et al., 2005; Zhang et al., 2009; Krugly et al., 2014). Concentrations of Nap in ambient air can range from 0.001 to 1.0 μg m^{-3} in typical suburban and urban environments (Price and Jayjock, 2008; Jia and Batterman, 2010; Batterman et al., 2012; Hamidin et al., 2013; Krugly et al., 2014), while significantly higher levels of Nap were observed at sites heavily affected by road traffics or near industrial emissions (Lu et al., 2005; Liu et al., 2007; Price and Jayjock, 2008; Uria-Tellaetxe et al., 2016). A recent study in Beijing during a winter haze period indicated that Nap and MN could contribute ~15% of SOA, which was comparable to that from single-ring aromatics including benzene, toluene and C_8 aromatics (Huang et al., 2019). Therefore, without considering the roles of Nap and MN as SOA precursors, previous studies might underestimate anthropogenic SOA from aromatics (Ding et al., 2012; Wu and Xie, 2018). The techniques commonly used for measuring VOCs and PAHs cannot be used satisfactorily for quantifying Nap and MN due to low recovery, hence the Nap and MN were generally missed in field measurements of both VOCs and PAHs (Yu et al., 2016; Zhang et al., 2018).

Nap and MN in ambient air are emitted from a range of anthropogenic sources, such as combustion of fossil fuels, biomass burning and industrial emission (Yuan et al., 2008; Lu et al., 2009; Zhao et al., 2015, 2016; Huang et al., 2018). According to global emission inventory of PAHs, combustion was considered as the main source of Nap (Zhang et al., 2009). Nap was also used as a combustion tracer for vehicle emission in previous studies on sources of VOCs in ambient air (Batterman et al., 2012; Uria-Tellaetxe et al., 2016). However, the major sources and their specific contributions to ambient Nap and MN are still poorly constrained. Field measurements of ambient Nap and MN can help narrow the uncertainty in their emission inventories and constrain results from model predictions. Given the fact that Nap and MN are important precursors of SOA, quantifying their emission sources in ambient air could help formulate effective air pollution control strategies.

In this study, ambient Nap and MN were measured in urban Guangzhou, a megacity in the Pearl River Delta (PRD) region of south China. In this region, primary organic aerosol (POA) in fine particles decreased significantly, yet the decreasing trend was not observed for SOA (Fu et al., 2014). A recent emission inventory of S/IVOCs in the PRD regions suggested IVOCs could contribute substantially to SOA in the region (Wu et al., 2019). It is necessary to explore and verify the emission sources of IVOCs in order to formulate air pollution control policies to modulate SOA in ambient air. Since Nap and MN are an important class of IVOCs, this study aimed to characterize Nap and MN as understudied SOA precursors in ambient air, to clarify their contributions to SOA relative to single-ring aromatic hydrocarbons, and to quantify their source contribution percentages along with measured VOCs. The results would provide useful information to modulate SOA in fine particles for further alleviating air pollution in the PRD region or in other megacities.

2. Experiments and methods

2.1. Field sampling

The field sampling was conducted from September 23rd to October 4th, 2019 on the top of a nine-story building (~30 m above the ground) in the campus of Guangzhou Institute of Geochemistry (23.12 °N, 113.36 °E; Fig. 1), Chinese Academy of Science in urban Guangzhou. Ambient Nap and MN were collected by sampling ambient air through a 47-mm polytetrafluoroethylene (PTFE) filter (Whatman, Maidstone, UK) followed by a sorption tube (Tenax TA/Carbograph 5TD, Markes International Ltd, UK). The PTFE filter was used to remove particles. The ambient air samples were collected by an automatic sampler (Model JEC921, Jectec Science and Technology, Co., Ltd, Beijing, China) at a flow rate of 0.6 L min^{-1} during time intervals of 8:00–9:00, 10:00–11:00, 12:00–13:00, 14:00–15:00, 16:00–17:00 and 18:00–19:00 local time, respectively. VOCs samples were also collected concurrently with 2 L stainless steel canisters through a model 910 canister sampler (Xonteck Inc., California, USA) at a flow rate of 66.7 mL min^{-1}. Three samples (18:00–19:00 on September 29th, 16:00–17:00 on October 1st, and 18:00–19:00 on October 3rd) were not collected because of unexpected power failure. Totally, 69 sorption tube samples and 69 canister samples were obtained during the campaign. The meteorological data including temperature (T, °C), relative humidity (RH, %), wind speed (WS, m s^{-1}), wind direction (WD, °) at the sampling site were obtained through an automatic weather station (Vantage Pro2, Davis Instruments Corp., USA). NOx were measured by an online trace gas analyzer (Model 42i-TL, Thermo Scientific, USA). The data of atmospheric boundary layer height (BLH) were obtained from NOAA's READY Archived Meteorology (http://ready.arl.noaa.gov/READYamet.php). 72-h backward trajectories of air masses were derived by Hybrid Single-Particle Lagrangian Integrated Trajectory model (HYSPLIT 4.0, https://ready.arl.noaa.gov/HYSPLIT.php).

2.2. Laboratory analysis

The sorption tubes were analyzed for Nap and MN with a gas chromatography (GC)/mass selective detector (MSD) (Agilent, 7890 GC/5975 MSD, USA) equipped with a thermal desorption system (TD-100, Markes International Ltd, UK). Prior to the thermal desorption, deuterated standard, naphthalene-d_8, was spiked into the sampled tubes to determine the recoveries of Nap and MN during the analysis.

Both sampled tubes and field blanks were thermally desorbed at 320 °C at 50 mL min^{-3} for 20 min. Then all desorbed analytes were transferred by pure helium into a cryogenic trap at −10 °C before the trap was rapidly heated to transfer the compounds to the GC/MSD system with a capillary column (Agilent, HP-5MS, 30 m × 0.25 mm × 0.25 μm). The temperature of transfer line was set at 250 °C. The GC oven temperature was initially at 60 °C, held for 2 min, then increased to 290 °C at 5 °C min^{-1} and kept for 20 min at 290 °C. The GC column was operated at a constant helium flow of 1.2 mL min^{-1}. The MS was run in the SCAN mode with electron impact ionization at 70 eV. Nap and MN were identified based on their retention times and mass spectra (Fig. S1), and were quantified by an internal standard method, which was described in detail in supporting information (Text S1).

The canister samples were used for analyzing the VOCs through a model 7100 pre-concentrator (Entech Instruments, California, USA) coupled with an Agilent 5973N gas chromatography mass selective detector flame ionization detector (GC-MSD/FID, Agilent Technologies,

USA). Detailed analysis for VOCs can be found elsewhere (Zhang et al., 2016, 2018).

2.3. Quality assurance and quality control (QA/QC)

Before sampling, the sorption tubes were conditioned by using clean carrier gas (high purity nitrogen, 99.999%) at a flow of 100 mL min^{-1} for 30 min at 330 °C followed by 1 h at 320 °C. Once cleaned, these tubes were sealed with brass storage caps fitted with combined PTFE ferrules. The cleaned tubes were wrapped in aluminum foil and the brass storage caps were not removed until immediately prior to sampling.

At the start and the end of sampling, the flow rate of the pump was calibrated by a soap-membrane flowmeter (Gilian Gilibrator-2, Sensidyne, USA). After sampling, the sorption tubes were stored at −20 °C in a freezer. During the campaign, five field blanks were collected with the sorption tubes being installed for 1 h but with the sampler pump off.

To check if any potential breakthrough exists during the sampling, two cleaned sorption tubes were connected in series to sample ambient air for 3 h, and then both were brought back to laboratory to be analyzed in the same way as field samples. The results revealed that Nap and MN in the second tubes were not detected or below their detection limits. Desorption recoveries were determined by analyzing the sorption tubes spiked with standards and d_8-naphthalene twice and calculated the percentage of targeted compounds in the first analysis. Desorption recoveries of 97%–100% were obtained in our study. Repeatability was evaluated by calculated the relative standard deviation (RSD) of 5 tubes injected with same level of standards, and results showed that the RSDs were below 10%. In this study, the method detection limits (MDLs) for Nap, 1-MN and 2-MN were 0.22 ng m^{-3}, 0.14 ng m^{-3} and 0.37 ng m^{-3}, respectively. Five field blanks and two laboratory blanks were analyzed in the same way as field samples, and Nap and MN were not detected or showed negligible levels below their MDLs in the blanks.

As for VOCs, the 2-L stainless steel canisters were cleaned by replicating filling and evacuating humidified zero air for at least five times. Then the cleaned canister filled with humidified zero air was analyzed in the same way as field samples to check if any compounds can be detected. The canisters could be used for VOCs sampling if no target compounds were detected or their levels were below their MDLs. An external calibration method was used for quantifying VOCs compounds (Zhang et al., 2016). Field blank canisters were refilled with zero air in the laboratory and then analyzed in the same way as filed samples. All target compounds in the field blanks were not detected.

2.4. Positive matrix factorization (PMF) model

USEPA PMF version 5.0 was employed in this study to resolve source contributions of ambient Nap and MN. The method is described in greater detail elsewhere (Paatero and Tapper, 1994; Paatero, 1997; Paterson et al., 1999). Briefly, data values below the method detection limits (MDLs) were substituted with MDL/2. The median concentrations were used for missing data values. If the concentration is less than or equal to the MDL used, the uncertainty is calculated using the equation of Unc = 5/6 × MDL. If the concentration is greater than MDL used, the uncertainty is calculated by Unc = $[(\text{Error Fraction} \times \text{concentration})^2 + (0.5 \times \text{MDL})^2]^{1/2}$. In this study, 44 species including Nap, 1-MN, 2-MN and 41 volatile organic compounds was input to the model. The model was run with the factors from 3 to 7 and a 4-factor resolution was selected (Text S2).

3. Results and discussion

3.1. Gas/particle partition and ambient levels

Nap and MN, as IVOCs that are less volatile than VOCs, might partition between gas and particulate phase. Detailed gas/particle partitioning of Nap and MN based on Pankow theory (Pankow, 1994a, b) during our field campaign was described in the supporting information (Text S3). As lower temperature and higher particle-bound OM would promote IVOCs to partition into particle-phase (Wang et al., 2016; Xie et al., 2013), the particle-bound Nap and MN were firstly calculated based on Pankow theory under the lowest temperature measured during the campaign (T = 24.6 °C; Fig. 2b). The results demonstrated that even under the lowest temperature, the calculated particle-phase concentrations for Nap, 1-MN and 2-MN were 1.52×10^{-3} ng m^{-3}, 4.54×10^{-4} ng m^{-3} and 9.56×10^{-4} ng m^{-3} (Table S1), respectively, which are several orders of magnitude lower and thus negligible when compared to their gas-phase concentrations (Table S1). The influence of OM on the gas/-particle partition was further evaluated by assuming that particle-bound

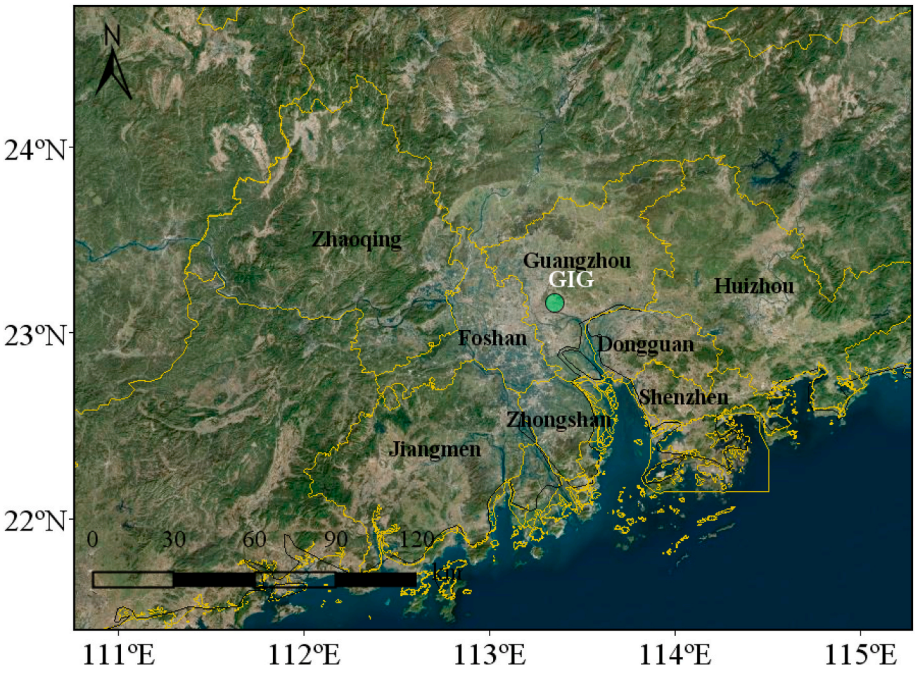

Fig. 1. The location of the sampling site, GIG, in the Pearl River Delta in south China.

OM were 6 μg m^{-3} higher or lower while keeping the temperature constant at 24.6 °C. In these cases calculated particle-bound concentrations of Nap, 1-MN and 2-MN ranged $6.90 \times 10^{-4} - 2.35 \times 10^{-3}$ ng m^{-3}, $2.06 \times 10^{-4} - 7.02 \times 10^{-4}$ ng m^{-3} and $4.34 \times 10^{-4} - 1.48 \times 10^{-3}$ ng m^{-3} (Table S1), respectively, which are also negligible relative to their gas-phase concentrations. Therefore, the particle-bound Nap and MN due to gas/particle partition in this study were not considered.

During the sampling period, the measured concentrations of Nap, 2-MN and 1-MN were 94.0 ± 23.1, 25.3 ± 4.5 and 11.8 ± 2.1 ng m^{-3} (mean ± 95% C.I.) (Fig. 2d and Table S2), respectively. The highest Nap concentration observed in this study reached 490 ng m^{-3}. The measured Nap concentrations in this study were within the range of 10–820 ng m^{-3} reported for ambient Nap levels in suburban and urban areas in countries including the US and Canada (Jia and Batterman, 2010), but much lower than that reported in the northern Beijing-Tianjin--Shijiazhuang (BTH) region (730 ± 310 ng m^{-3}) in China. The lower ambient Nap concentrations in Guangzhou than in the BTH region were also reported in a previous study by Tang et al. (2020). However, when compared to the Nap concentrations measured in Guangzhou in 2018 by Tang et al. (2020), the average concentration of Nap in this study in autumn (September and October) was higher than that of 70 ± 20 ng m^{-3} in summer and spring in 2018, but lower than that of 220 ± 50 ng m^{-3} in winter in 2018. Apart from relatively higher boundary layer height (BLH) in summer but lower BLH in winter (Table S3), the change in monsoons might be a reason for the difference in ambient Nap levels. As indicated by Tang et al. (2020), 72-h back trajectories revealed that about 39%, 60% and 100% of air masses were oceanic in winter, spring and summer, respectively, while during our sampling period 44.7% were ocean air masses (Fig. S5) with less anthropogenic impacts and lower Nap concentrations. However, these levels were significantly higher than that of <10 ng m^{-3} in Guangzhou as reported over a decade ago by Li et al. (2006) and Yang et al. (2010), implying increasing

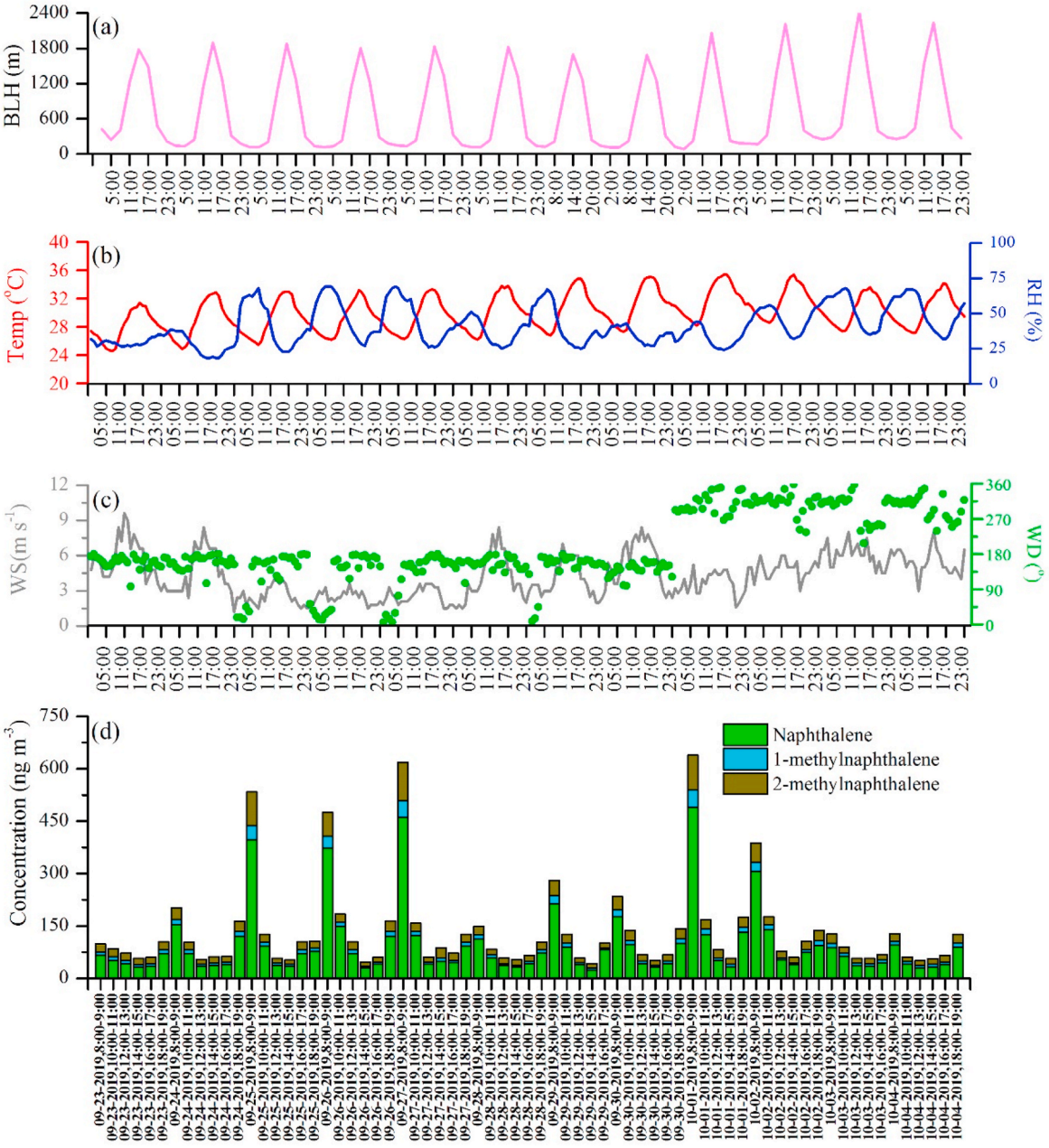

Fig. 2. The temporal variations of (a) boundary layer height (BLH), (b) temperature (Temp), relative humidity (RH), (c) wind speed (WS), wind direction (WD) and (d) Nap and MN concentrations during the sampling period.

anthropogenic contributions of these IVOCs in recent years.

Measured concentrations of MN changed in similar trends to that of Nap, as reflected by the significant positive correlations between 1-MN and 2-MN ($R^2 = 0.97$, $p < 0.01$), and between Nap and MN ($R^2 = 0.95$, $p < 0.01$) (Fig. S6). The daily averages of Nap + MN during the campaign (Fig. S7) showed significantly higher ambient levels during September 25th-27th and October 1st-2nd, possibly due to lower wind speeds, which were unfavorable for the dispersion of air pollutants (Fig. 2c). As for the diurnal variations, relatively higher concentrations of Nap and MN were measured at 8:00–9:00 and 18:00–19:00 (Fig. S8), while lower concentrations occurred during 12:00–15:00 in the afternoon. This might be related to the temporal variations of BLH, which were generally lower before 9:00 and after 17:00, but were higher during 10:00–16:00 (Fig. 2a). More importantly, vehicles emissions at rush-hours and strong photochemical degradation at noon time could be the reasons for the peak levels during 8:00–9:00 and 18:00–19:00, and the lower levels during 10:00–16:00 (Jia and Batterman, 2010; Wang et al., 2013).

3.2. Photochemical ageing and initial concentrations

As mentioned above, photochemical reactions could result in lower concentrations of Nap and MN observed during 12:00–16:00. Previous studies suggested that, due to photochemical consumptions, in-situ observed VOCs could not reflect those released from various sources, and this would influence the accuracy of sources apportionment by receptor modelling using the observed ambient VOCs data (Shao et al., 2009; Yuan et al., 2012; Wang et al., 2013; He et al., 2019). Photochemical processes would certainly impact on in-situ measured concentrations of Nap and MN since they can be consumed by OH radicals in ambient air (Atkinson and Arey, 2003). The initial concentrations of Nap and MN could be also derived considering photochemical aging under OH exposure, which can be calculated by the ratio of two VOC species, ethylbenzene (E) and m/p-xylenes (X) (Nelson and Quigley, 1983). The two VOC species in this study showed highly significant correlation ($R^2 = 0.94$, $p < 0.01$) (Fig. S9), suggesting the similar sources shared by them. The initial concentrations of Nap and MN were thus calculated by following equations (de Gouw et al., 2005; Parrish et al., 2007; Shao et al., 2009; Zhang et al., 2016):

$$[S_i]_{observed} = [S_i]_{initial} \times \exp(-k_i[OH]\Delta t) \quad (1)$$

$$[OH]\Delta t = \frac{1}{k_E - k_X} \times \left(\ln\left\{\frac{[E]}{[X]}|_{t=t_0}\right\} - \ln\left\{\frac{[E]}{[X]}|_{t=t}\right\}\right) \quad (2)$$

where $[S_i]_{observed}$ and $[S_i]_{initial}$ are the observed and initial concentrations of Nap or MN, respectively; k_i represents the reaction rate constant of Nap or MN with OH radicals; k_E and k_X represents the reaction rate constant of ethylbenzene and m/p-xylenes with OH radicals, respectively; $[OH]$ is the concentration of the OH radicals, and Δt is the reaction time or the photochemical age; $\frac{[E]}{[X]}|_{t=t}$ represents the concentration ratio of measured ethylbenzene to m/p-xylenes at time t, while $\frac{[E]}{[X]}|_{t=t_0}$ represents the initial concentration ratio of ethylbenzene to m/p-xylenes. Here, 0.5 was chosen as the initial ratio of ethylbenzene to m/p-xylenes based on our observations (data not reported here) in urban Guangzhou in early morning (00:00–4:00 a.m.). This initial emission ratio was also adopted in a previous study in the PRD region (Wang et al., 2016), and was comparable to that used in other typical cities like Beijing and Shanghai (Shao et al., 2009; Wang et al., 2013).

The calculated average total initial concentrations for Nap and MN was 337.8 ± 79.6 ng m^{-3} (Table S2), ~2.6 times higher than the measured average. The highest total initial concentration could reach 1772 ng m^{-3}. Fig. 3 shows the comparison of measured and initial concentrations of Nap and MN, as well as those for single-ring aromatics including benzene, toluene, C8 aromatics and C9 aromatics. The single-ring aromatics are among the most abundant VOCs and have been considered as the most important anthropogenic SOA precursors in most urban areas (Liu et al., 2009; Cai et al., 2010; Ding et al., 2012; Boynard et al., 2014; Borbon et al., 2018; Wu and Xie, 2018; Dominutti et al., 2019). The ratios of initial to observed concentration at time intervals of 12:00–13:00 and 14:00–15:00 were the ones when photochemical aging influenced more strongly. As showed in Fig. 3, the initial/observed ratios of Nap and MN were higher than that of single-ring aromatics except for styrene and 1,3,5-trimethybenzene. The ratios of initial to observed concentration for 2-MN, 1-MN and Nap were consistent with their reaction rate constants with OH radicals, $k_{2\text{-}MN} > k_{1\text{-}MN} > k_{Nap}$ (Fig. 3; Table S4). The higher ratios of initial/observed of Nap and MN relatively to most of single-ring aromatics indicated that they were easier to be consumed by atmospheric oxidants to produce SOA (Wang et al., 2020).

3.3. SOA formation from Nap and MN

The contributions of Nap, MN and single-ring aromatics oxidations to SOA formation was estimated by the consumed precursor concentrations and their SOA yields during the strong photochemical period (12:00–15:00) as below (Yuan et al., 2013; Huang et al., 2019):

$$\Delta[S_i] = [S_i]_{initial} - [S_i]_{observed} = [S_i]_{initial} \times (1 - \exp(-k_i[OH]\Delta t)) \quad (3)$$

$$SOA_{i\,estimated} = \Delta[S_i] \times Yield_i \quad (4)$$

where $\Delta[S_i]$ represents the consumed concentrations of Nap, MN and BTEX. $\boldsymbol{SOA}_{i,\ estimated}$ is the SOA production estimated from precursor $\boldsymbol{i}$. $\boldsymbol{Yield}_i$ represents the SOA yield of precursor $\boldsymbol{i}$ which were determined from previous chamber studies (Table S5). NOx concentration can significantly affect SOA yields (Presto et al., 2005; Lee et al., 2006; Ng et al., 2007). The ratio of VOCs to NOx was used to determine NOx level conditions (Lane et al., 2008; Wu and Xie, 2018): VOCx/NOx > 10 as low-NOx condition and VOCs/NOx < 3 as high-NOx conditions. During the campaign in this study, the ratio of VOCs/NOx was 1.76 ± 0.30 with a maximum of 5.58 (Table S6). Therefore, SOA yields under the high-NOx conditions were used in this study (Table S5).

As shown in Fig. 4a, the total estimated SOA from Nap, MN and single-ring aromatics was 0.49 μg m^{-3}, and Nap + MN accounted for 12.4% of the SOA mass formed during the strong photochemical periods. C8 aromatics (Ethylbenzene, Xylenes and Styrene) with the highest

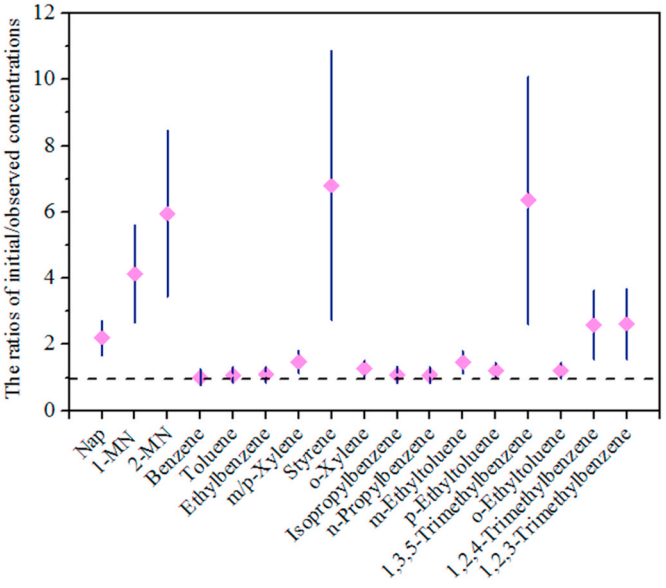

Fig. 3. Ratios of initial to observed concentrations for Nap, MN and BTEX. The error bars represent 95% confident interval (95% C.I.). The dashed line represents ratio of one.

emission among the precursors was also the greatest contributor of estimated SOA (Fig. 4). Although the initial levels of Nap and MN were less than 2% of single-ring aromatics (Fig. 4b), their contributions to SOA were comparable to that from toluene or C9 aromatics, largely due to relatively higher SOA yields and faster oxidation rates of Nap and MNs. Similar results were also found in a field campaign conducted in Beijing during a winter haze, when Nap + MN with less than 8% of single-ring aromatics in emissions could contribute 38.2% of SOA mass from Nap, MN and single-ring aromatics (Huang et al., 2019). Chamber studies also have revealed that Nap and MN were important SOA precursors in gasoline exhaust and 8%–52% SOA formation was contributed by Nap (Liu et al., 2015). While Nap and MN have reported to be less 30% of single-ring aromatics both in diesel exhaust and in pine wood burning plume, they could contribute 1.3 times and 3.2 times SOA formed from single-ring aromatics in diesel exhaust and pine wood burning plume, respectively (Chan et al., 2009). These findings suggest that Nap and MN are also important anthropogenic SOA precursors along with aromatic hydrocarbons, although their emissions might be substantially lower than aromatic hydrocarbons.

3.4. Sources of Nap and MN

Given that Nap and MN in ambient air were heavily influenced by photochemical ageing especially at noon, the PMF model was applied to explore their source contributions with a photochemical age-based calculation of the initial concentrations as described above in section 3.2. The initial concentrations of 44 species, including Nap, 1-MN, 2-MN and 41 VOCs, were input into the model.

Fig. 5 displays the source profiles resolved by the PMF model. Factor 1 is characterized with high load of ethane, ethylene and chloromethane. Chloromethane is a typical marker of biomass burning (Liu et al., 2008; Huang et al., 2017; Yang et al., 2018), and ethane and ethylene were found with large percentages in rice straw burning and coal burning (Zhang et al., 2013, 2013; Fang et al., 2017). Therefore, this factor is considered as biomass/coal burning. Factor 2 is featured by abundant n-undecane and n-dodecane. More long-chain hydrocarbons and relatively higher percentages of alkenes suggests this factor could be diesel vehicle emission (Watson et al., 2001; Song et al., 2007; Guo et al., 2011; Ou et al., 2014; Zhao et al., 2015). Factor 3 is characterized by abundant C_6–C_7 alkanes and aromatics like toluene. These compounds are commonly used in the industrial processes (Chan et al., 2006; Ou et al., 2015). In addition, much less loading of MN is found in this factor. This may suggest that the factor 3 is associated with industrial emission. As Nap is used for the productions of phthalic anhydride, surfactants and pesticides (Jia and Batterman, 2010), Nap can also present in this factor. Factor 4 is demonstrated with high percentage of C_5–C_6 alkanes, which are considered as gasoline vehicle emissions (Chang et al., 2006; Zhang et al., 2015; Yang et al., 2018). 2,2-dimethylbutane, which is used for increasing the octane level of gasoline (Chang et al., 2004, 2006), is also found to be abundant in this factor. Hence, factor 4 is related to gasoline vehicle emission.

Fig. 6 shows the relative contributions to ambient Nap + MN from the resolved sources. Gasoline exhaust ranked the first with a contribution percentage of 39.1% to ambient Nap and MN, followed by biomass/coal burning (29.9%), diesel exhaust (26.3%) and industrial emission (4.7%). Therefore, vehicle exhaust (diesel + gasoline) was the major source (~65%) of ambient Nap and MN during the campaign in this study. Fig. S10 demonstrates the diurnal variations of Nap + MN by different sources extracted from the PMF model. Compared to vehicle emissions, the biomass burning and industrial emission showed much smaller diurnal fluctuations, similar to results reported previously (He et al., 2019).

A previous study in Guangzhou has reported coal combustion was the largest contributor (43.4%) to ambient Nap (Tang et al., 2020), followed by liquid fossil combustion (mainly motor vehicle exhaust) (40.0%) and biomass burning (16.6%). The result is quite different from that obtained in this study, particularly in the contribution of biomass/coal burning, which is only ~20% in this study (Fig. S11) while coal combustion alone contributed over 40% to Nap in the study by Tang et al. (2020). There are several reasons for the difference. Firstly, only three sources (liquid fossil fuel, coal burning and biomass burning) based on emission inventory of PAHs were considered in the study by Tang et al. (2020). However, industrial activities may also give emissions to Nap (Jia and Batterman, 2010) although this source might have a minor contribution. Secondly, Nap is a highly reactive species with a lifetime of ~12 h under a normal OH radical concentration of 1×10^6 molecule^{-1} cm^{-3} s^{-1}. The Nap levels obtained by Tang et al. (2020) with 24-h Nap sampling might be far less than its initial values as calculated in this study, and directly using the measured levels from 24-h sampling in the model for source apportioning might bias toward greater contributions by coal burning. As a matter of fact, the sampling site in Tang et al. (2020) and this study is located in a coal-free district, where coal-burning is forbidden in both residential and industrial uses.

With the source apportionment results, the total SOA formation potentials (SOAFP) by the single- and two-ring aromatics from different sources can be further estimated. As showed in Table S7, the industrial

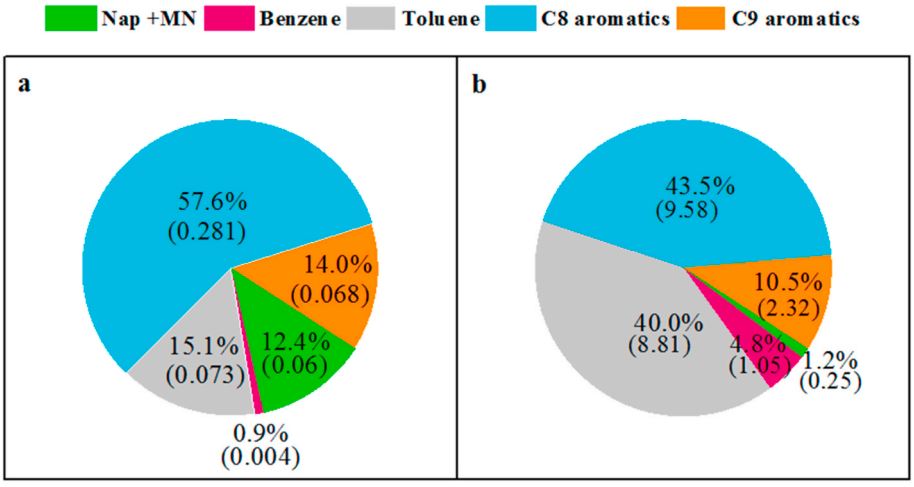

Fig. 4. Contributions to estimated SOA (a) and initial concentrations (b) of Nap + MN and single-ring aromatics during the periods strongly influenced by photochemical reaction (12:00–13:00 and 14:00–15:00). The values in brackets represent SOA productions (a) and initial concentrations of precursors (b) (in μg m^{-3}).

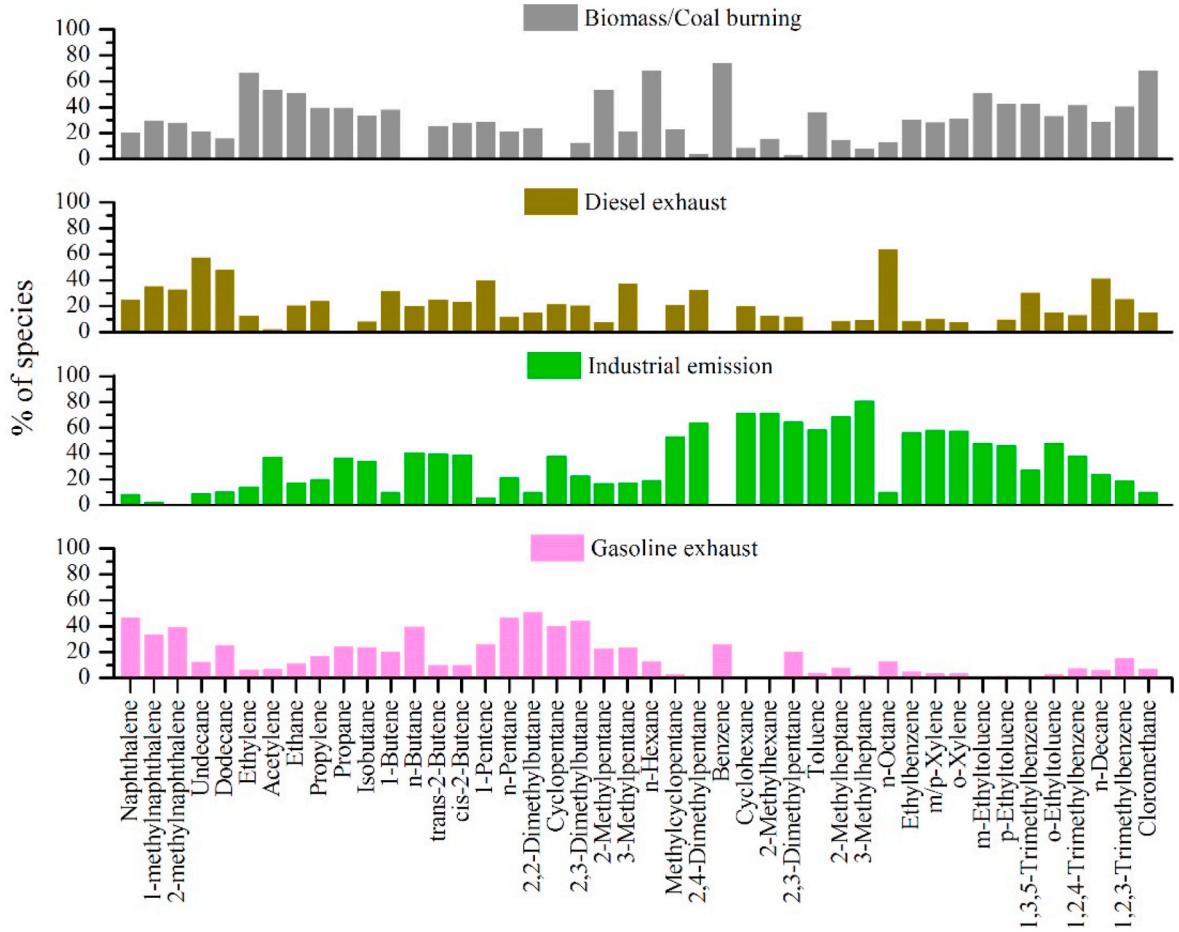

Fig. 5. Source profiles resolved by the PMF model.

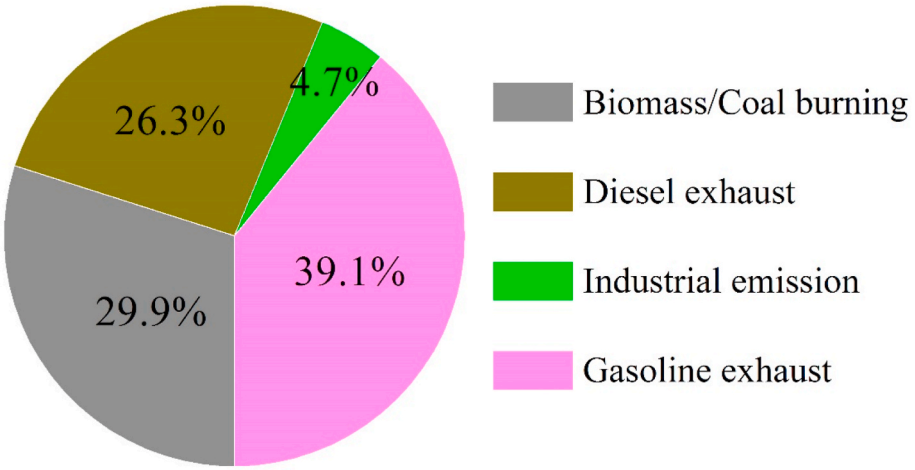

Fig. 6. Source contributions to ambient Nap and MN by different sources during the campaign.

emission was the largest contributor (0.85 ± 0.20 μg m^{-3}), accounting for ~ 50% of total SOAFP. This was mainly attributed to substantial emissions of sing-ring aromatics from industrial activities (Zhang et al., 2013, 2013; He et al., 2019). A previous study based on VOCs emission inventory also revealed that surface coating in the PRD region was the largest contributor to SOAFP (Wu et al., 2018). The biomass/coal burning contributed a slightly lower SOAFP (0.67 ± 0.13 μg m^{-3}) than industrial emission, but much higher when compared to that of 0.14 ± 0.02 μg m^{-3} by gasoline exhaust or 0.10 ± 0.02 μg m^{-3} by diesel exhaust. Estimated SOAFPs of the two-ring Nap and MN from the above four sources, however, were quite different. Vehicle emission and biomass/coal burning became important contributors while contribution by industrial emission was negligible. As Nap and MN are a typical class of IVOCs, this significant difference suggested that IVOCs should be taken into consideration when we explore the SOA formation by precursors from different sources.

4. Conclusions

Ambient Nap and MN were measured at an urban site in the PRD region from September 23rd to October 4th, 2019. Measured concentrations of Nap, 2-MN and 1-MN during the campaign were 94.0 ± 23.1, 25.3 ± 4.5 and 11.8 ± 2.1 ng m^{-3}, respectively. Diurnal variations in concentrations of Nap and MN might be attributed to rush-hour vehicle emissions, stronger photochemical reaction in the afternoon and changes in BLH. Calculated initial concentrations of Nap and MN by a photochemical age-based parameterization method were ~2.6 times higher than the directly observed ones. While initial concentrations of Nap and MN were less than 2% of that of single-ring aromatics during 12:00–15:00, they could contribute about 12.4% of estimated SOA from Nap, MN and single-ring aromatics. The PMF model with initial concentrations of Nap, MN and VOCs was for the first time used for source apportioning of ambient Nap and MN. Gasoline vehicle emission was found to be the largest contributor to Nap and MN (39.1%), followed by biomass/coal burning (29.9%), diesel vehicles emission (26.3%) and industrial emission (4.7%). The total SOAFP by the single- and two-ring aromatics from different sources revealed that due to substantial emissions of single-ring aromatics, industrial emission was the largest contributor, accounting for ~50% of total SOAFP. This was different from the result that on-road vehicle contributed most to estimated SOAFP from Nap and MN.

The results of this study highlights the importance of Nap and MN as anthropogenic SOA precursors in urban areas, where traffic density is much higher and vehicle exhaust is a major source of Nap and MN as implied in this study. Although IVOCs like Nap and MN are important contributors in vehicle exhaust and biomass/coal burning, they are less represented or characterized in the emission tests either for particulate pollutants or gaseous pollutants. As reducing the emissions of IVOCs like Nap and MN might be of great importance in lowering SOA in $PM_{2.5}$ in urban areas, more studies on characterizing the emissions of these IVOCs, as well as more field works on their ambient levels and sources, would help understand these understudied SOA precursors and control their emissions for further alleviating fine particle air pollution in urban areas.

CRediT authorship contribution statement

Hua Fang: Investigation, Formal analysis, Methodology, Writing – original draft, Data curation. **Shilu Luo:** Investigation, Methodology. **Xiaoqing Huang:** Investigation, Methodology. **Xuewei Fu:** Investigation, Data curation. **Shaoxuan Xiao:** Investigation, Data curation. **Jianqiang Zeng:** Data curation. **Jun Wang:** Investigation. **Yanli Zhang:** Investigation, Data curation. **Xinming Wang:** Conceptualization, Supervision, Writing – review & editing, Funding acquisition.

Declaration of competing interest

The authors declare that they have no known competing financial interests or personal relationships that could have appeared to influence the work reported in this paper.

Acknowledgments

This study was funded by Natural Science Foundation of China (41530641/41961144029), the National Key Research and Development Program (2016YFC0202204/2017YFC0212802), the Chinese Academy of Sciences (QYZDJ-SSW-DQC032), and Department of Science and Technology of Guangdong Province (2017B030314057/2017BT01Z134/2019B121205006).

Appendix A. Supplementary data

Supplementary data to this article can be found online at https://doi.org/10.1016/j.atmosenv.2021.118295.

References

Atkinson, R., Arey, J., 2003. Atmospheric degradation of volatile organic compounds. Chem. Rev. 103, 4605e4638. https://doi.org/10.1021/cr0206420.

ATSDR, 2005. Toxicological Profile for Naphthalene, 1-methylnaphthalene, and 2-methylnaphthalene. U.S. Department of Health and Human Services, Agency for Toxic Substances and Disease Registry, Atlanta, GA, USA, pp. 1–291.

Batterman, S., Chin, J.Y., Jia, C., Godwin, C., Parker, E., Robins, T., Max, P., Lewis, T., 2012. Sources, concentrations, and risks of naphthalene in indoor and outdoor air. Indoor Air 22, 266–278. https://doi.org/10.1111/j.1600-0668.2011.00760.x.

Borbon, A., Boynard, A., Salameh, T., Baudic, A., Gros, V., Gauduin, J., Perrussel, O., Pallares, C., 2018. Is traffic still an important emitter of monoaromatic organic compounds in European urban areas? Environ. Sci. Technol. 52, 513–521. https://doi.org/10.1021/acs.est.7b01408.

Boynard, A., Borbon, A., Leonardis, T., Barletta, B., Meinardi, S., Blake, D.R., Locoge, N., 2014. Spatial and seasonal variability of measured anthropogenic non-methane hydrocarbons in urban atmospheres: implication on emission ratios. Atmos. Environ. 82, 258–267. https://doi.org/10.1016/j.atmosenv.2013.09.039.

Cai, C.J., Geng, F.H., Tie, X.X., Yu, Q., An, J.L., 2010. Characteristics and source apportionment of VOCs measured in Shanghai, China. Atmos. Environ. Times 44, 5005–5014. https://doi.org/10.1016/j.atmosenv.2010.07.059.

Chan, A.W.H., Kautzman, K.E., Chhabra, P.S., Surratt, J.D., Chan, M.N., Crounse, J.D., Kürten, A., Wennberg, P.O., Flagan, R.C., Seinfeld, J.H., 2009. Secondary organic aerosol formation from photooxidation of naphthalene and alkylnaphthalenes: implications for oxidation of intermediate volatility organic compounds (IVOCs). Atmos. Chem. Phys. 9, 3049–3060. https://doi.org/10.5194/acp-9-3049-2009.

Chan, L.Y., Chu, K.W., Zou, S.C., Chan, C.Y., Wang, X.M., Barletta, B., Blake, D.R., Guo, H., Tsai, W.Y., 2006. Characteristics of nonmethane hydrocarbons (NMHCs) in industrial, industrial-urban, and industrial-suburban atmospheres of the Pearl River Delta (PRD) region of south China. J. Geophys. Res. Atmos. 111, D11304. https://doi.org/10.1029/2005JD006481.

Chang, C.C., Chen, T.Y., Chou, C., Liu, S.C., 2004. Assessment of traffic contribution to hydrocarbons using 2,2-dimethylbutane as a vehicular indicator. Terr. Atmos. Ocean Sci. 15, 697–711. https://doi.org/10.3319/tao.2004.15.4.697(A).

Chang, C.C., Wang, J.J., Liu, S.C., Candice Lung, S.C., 2006. Assessment of vehicular and non-vehicular contributions to hydrocarbons using exclusive vehicular indicators. Atmos. Environ. 40, 6349–6361. https://doi.org/10.1016/j.atmosenv.2006.05.043.

Chen, C.L., Kacarab, M., Tang, P., Cocker, D.R., 2016. SOA formation from naphthalene, 1-methylnaphthalene, and 2-methylnaphthalene photooxidation. Atmos. Environ. 131, 424–433. https://doi.org/10.1016/j.atmosenv.2016.02.007.

de Gouw, J.A., Middlebrook, A.M., Warneke, C., Goldan, P.D., Kuster, W.C., Roberts, J. M., Fehsenfeld, F.C., Worsnop, D.R., Canagaratna, M.R., Pszenny, A.A.P., Keene, W. C., Marchewka, M., Bertman, S.B., Bates, T.S., 2005. Budget of organic carbon in a polluted atmosphere: results from the New England air quality study in 2002. J. Geophys. Res. Atmos. 110, D16305. https://doi.org/10.1029/2004jd005623.

Dey, S., Ballav, P., Samanta, P., Mandal, A., Das, S., Mondal, A.K., Ghosh, A.R., 2021. Time-dependent naphthalene toxicity in anabas testudineus (Bloch): a multiple endpoint biomarker approach. ACS Omega 6, 317–326. https://doi.org/10.1021/acsomega.0c04603.

Ding, X., Wang, X.M., Gao, B., Fu, X.X., He, Q.F., Zhao, X.Y., Yu, J.Z., Zheng, M., 2012. Tracer-based estimation of secondary organic carbon in the Pearl River Delta, south China. J. Geophys. Res. Atmos. 117, D05313. https://doi.org/10.1029/2011JD016596.

Dominutti, P., Keita, S., Bahino, J., Colomb, A., Liousse, C., Yoboué, V., Galy-Lacaux, C., Morris, E., Bouvier, L., Sauvage, S., Borbon, A., 2019. Anthropogenic VOCs in Abidjan, southern West Africa: from source quantification to atmospheric impacts. Atmos. Chem. Phys. 19, 11721–11741. https://doi.org/10.5194/acp-19-11721-2019.

Fang, Z., Deng, W., Zhang, Y., Ding, X., Tang, M., Liu, T., Hu, Q., Zhu, M., Wang, Z., Yang, W., Huang, Z., Song, W., Bi, X., Chen, J., Sun, Y., George, C., Wang, X., 2017. Open burning of rice, corn and wheat straws: primary emissions, photochemical aging, and secondary organic aerosol formation. Atmos. Chem. Phys. 17, 14821–14839. https://doi.org/10.5194/acp-17-14821-2017.

Fu, X.X., Wang, X.M., Guo, H., Cheung, K., Ding, X., Zhao, X.Y., He, Q.F., Gao, B., Zhang, Z., Liu, T.Y., Zhang, Y.L., 2014. Trends of ambient fine particles and major chemical components in the Pearl River Delta region: observation at a regional background site in fall and winter. Sci. Total Environ. 497–498, 274–281. https://doi.org/10.1016/j.scitotenv.2014.08.008.

Guo, H., Cheng, H.R., Ling, Z.H., Louie, P.K.K., Ayoko, G.A., 2011. Which emission sources are responsible for the volatile organic compounds in the atmosphere of Pearl River Delta? J. Hazard Mater. 188, 116–124. https://doi.org/10.1016/j.jhazmat.2011.01.081.

Hamidin, N., Yu, J., Phung, D.T., Connell, D., Chu, C., 2013. Volatile aromatic hydrocarbons (VAHs) in residential indoor air in Brisbane, Australia. Chemosphere 92, 1430–1435. https://doi.org/10.1016/j.chemosphere.2013.03.050.

He, Z.R., Wang, X.M., Ling, Z.H., Zhao, J., Guo, H., Shao, M., 2019. Contributions of different anthropogenic volatile organic compound sources to ozone formation at a receptor site in the Pearl River Delta region and its policy implications. Atmos. Chem. Phys. 19, 8801–8816. https://doi.org/10.5194/acp-19-8801-2019.

Huang, C., Hu, Q.Y., Li, Y.J., Tian, J.J., Ma, Y.G., Zhao, Y.L., Feng, J.L., An, J.Y., Qiao, L. P., Wang, H.L., Jing, S.A., Huang, D.D., Lou, S.R., Zhou, M., Zhu, S.H., Tao, S.K., Li, L., 2018. Intermediate volatility organic compound emissions from a large cargo

vessel operated under real-world conditions. Environ. Sci. Technol. 52, 12934–12942. https://doi.org/10.1021/acs.est.8b04418.
Huang, G.C., Liu, Y., Shao, M., Li, Y., Chen, Q., Zheng, Y., Wu, Z.J., Liu, Y.C., Wu, Y.S., Hu, M., Li, X., Lu, S.H., Wang, C.J., Liu, J.Y., Zheng, M., Zhu, T., 2019. Potentially important contribution of gas-phase oxidation of naphthalene and methylnaphthalene to secondary organic aerosol during haze events in Beijing. Environ. Sci. Technol. 53, 1235–1244. https://doi.org/10.1021/acs.est.8b04523.
Huang, X.Y., Zhang, Y.L., Yang, W.Q., Huang, Z.Z., Zhang, Z., He, Q.F., Lü, S.J., Huang, Z.H., Bi, X.H., 2017. Effect of traffic restriction on reducing ambient volatile organic compounds (VOCs): observation-based evaluation during a traffic restriction drill in Guangzhou, China. Atmos. Environ. 161, 61–70. https://doi.org/10.1016/j.atmosenv.2017.04.035.
Jia, C., Batterman, S., 2010. A critical review of naphthalene sources and exposures relevant to indoor and outdoor air. Int. J. Environ. Res. Publ. Health 7, 2903–2939. https://doi.org/10.3390/ijerph7072903.
Krugly, E., Martuzevicius, D., Sidaraviciute, R., Ciuzas, D., Prasauskas, T., Kauneliene, V., Stasiulaitiene, I., Kliucininkas, L., 2014. Characterization of particulate and vapor phase polycyclic aromatic hydrocarbons in indoor and outdoor air of primary schools. Atmos. Environ. 82, 298e306. https://doi.org/10.1016/j.atmosenv.2013.10.042.
Lane, T.E., Donahue, N.M., Pandis, S.N., 2008. Effect of NOx on secondary organic aerosol concentrations. Environ. Sci. Technol. 42, 6022–6027. https://doi.org/10.1021/es703225a.
Lee, A., Goldstein, A.H., Keywood, M.D., Gao, S., Varutbangkul, V., Bahreini, R., Ng, N. L., Flagan, R.C., Seinfeld, J.H., 2006. Gas-phase products and secondary aerosol yields from the ozonolysis of ten different terpenes. J. Geophys. Res. Atmos. 111, D17. https://doi.org/10.1029/2005jd006437.
Li, J., Zhang, G., Li, X.D., Qi, S.H., Liu, G.Q., Peng, X.Z., 2006. Source seasonality of polycyclic aromatic hydrocarbons (PAHs) in a subtropical city, Guangzhou, South China. Sci. Total Environ. 355, 145–155. https://doi.org/10.1016/j.scitotenv.2005.02.042.
Lin, C.Y., Wheelock, Åsa M., Morin, D., Baldwin, R.M., Lee, M.G., Taff, A., Plopper, C., Buckpitt, A., Rohde, A., 2009. Toxicity and metabolism of methylnaphthalenes: comparison with naphthalene and 1-nitronaphthalene. Toxicology 260, 16–27. https://doi.org/10.1016/j.tox.2009.03.002.
Liu, J.F., Mu, Y.J., Zhang, Y.J., Zhang, Z.M., Wang, X.K., Liu, Y.J., Sun, Z.Q., 2009. Atmospheric levels of BTEX compounds during the 2008 Olympic Games in the urban area of Beijing. Sci. Total Environ. 408, 109–116. https://doi.org/10.1016/j.scitotenv.2009.09.026.
Liu, T.Y., Wang, X.M., Deng, W., Hu, Q., Ding, X., Zhang, Y.L., He, Q.F., Zhang, Z., Lü, S. J., Bi, X.H., Chen, J.M., Yu, J.Z., 2015. Secondary organic aerosol formation from photochemical aging of light-duty gasoline vehicle exhausts in a smog chamber. Atmos. Chem. Phys. 15 https://doi.org/10.5194/acp-15-9049-2015, 9094-9062.
Liu, Y., Shao, M., Fu, L.L., Lu, S.H., Zeng, L.M., Tang, D.G., 2008. Source profiles of volatile organic compounds (VOCs) measured in China: Part I. Atmos. Environ. 42, 6247–6260. https://doi.org/10.1016/j.atmosenv.2008.01.070.
Liu, Y.A., Tao, S., Yang, Y.F., Dou, H., Yang, Y., Coveney, R.M., 2007. Inhalation exposure of traffic police officers to polycyclic aromatic hydrocarbons (PAHs) during the winter in Beijing. Sci. Total Environ. 2007 https://doi.org/10.1016/j.scitotenv.2007.05.008.
Loh, M.M., Levy, J.I., Spengler, J.D., Houseman, E.A., Bennett, D.H., 2007. Ranking cancer risks of organic hazardous air pollutants in the United States. Environ. Health Perspect. 115, 1160–1168. https://doi.org/10.1289/ehp.9884.
Lu, H., Zhu, L., Zhu, N., 2009. Polycyclic aromatic emission from straw burning and the influence of combustion parameters. Atmos. Environ. 43, 978–983. https://doi.org/10.1016/j.atmosenv.2008.10.022.
Lu, R., Wu, J., Turco, R.P., Winer, A.M., Atkinson, R., Arey, J., Paulson, S.E., Lurmann, F. W., Miguel, A.H., Eiguren-Fernandez, A., 2005. Naphthalene distributions and human exposure in southern California. Atmos. Environ. 39, 489–507. https://doi.org/10.1016/j.atmosenv.2004.09.045.
Lundstedt, S., White, P.A., Lemieux, C.L., Lynes, K.D., Lambert, I.B., Öberg, L., Haglund, P., Tysklind, M., 2007. Sources, fate, and toxic hazards of oxygenated polycyclic aromatic hydrocarbons (PAHs) at PAH-contaminated sites. Ambio 36, 475–485. https://doi.org/10.1579/0044-7447(2007)36[475:SFATHO]2.0.CO;2.
Nelson, P.E., Quigley, S.M., 1983. The m, p-xylene/ethylbenzene ratio: a technique for estimating hydrocarbon age in ambient atmosphere. Atmos. Environ. 17, 659–662. https://doi.org/10.1016/0004-6981(83)90141-5.
Ng, N.L., Kroll, J.H., Chan, A.W.H., Chhabra, P.S., Flagan, R.C., Seinfeld, J.H., 2007. Secondary organic aerosol formation from m-xylene, toluene, and benzene. Atmos. Chem. Phys. 7, 3909–3922. https://doi.org/10.5194/acp-7-3909-2007.
Ou, J.M., Feng, X.Q., Liu, Y.C., Gao, Z.Z., Yang, Y., Zhou, Z., Wang, X.M., Zheng, J.Y., 2014. Source characteristics of VOCs emissions from vehicular exhaust in the Pearl River Delta region. Acta Sci. Circumstantiae 34, 826–834. https://doi.org/10.13671/j.hjkxxb.2014.0614.
Ou, J.M., Guo, H., Zheng, J.Y., Cheung, K., Louie, P.K.K., Ling, Z.H., Wang, D.W., 2015. Concentrations and sources of nonmethane hydrocarbons (NMHCs) from 2005 to 2013 in Hong Kong: a multi-year real-time data analysis. Atmos. Environ. 103, 196–206. https://doi.org/10.1016/j.atmosenv.2014.12.048.
Paatero, P., 1997. Least squares formulation of robust non-negative factor analysis. Chemom. Intell. Lab. 37, 23–35. https://doi.org/10.1016/S0169-7439(96)00044-5.
Paatero, P., Tapper, U., 1994. Positive matrix factorization - a nonnegative factor model with optimal utilization of error-estimates of data values. Environmetrics 5, 111–126. https://doi.org/10.1002/env.3170050203.
Pankow, J.F., 1994a. An absorption-model of gas-particle partitioning of organic compounds in the atmosphere. Atmos. Environ. 28, 185–188. https://doi.org/10.1016/1352-2310(94)90093-0.
Pankow, J.F., 1994b. An absorption-model of the gas/aerosol partitioning involved in the formation of secondary organic aerosol. Atmos. Environ. 28, 189–193. https://doi.org/10.1016/j.atmosenv.2007.10.060.
Parrish, D.D., Forster, A.C., Atlas, E.L., Blake, D.R., Goldan, P.D., Kuster, W.C., de Gouw, J.A., 2007. Effects of mixing on evolution of hydrocarbon ratios in the troposphere. J. Geophys. Res. Atmos. 112, D10S34. https://doi.org/10.1029/2006JD007583.
Paterson, K.G., Sagady, J.L., Hooper, D.L., 1999. Analysis of air quality data using positive matrix factorization. Environ. Sci. Technol. 33, 635–641. https://doi.org/10.1021/Es980605j.
Presto, A.A., Hartz, K.E.H., Donahue, N.M., 2005. Secondary organic aerosol production from terpene ozonolysis. 2. Effect of NOx concentration. Environ. Sci. Technol. 39, 7046–7054. https://doi.org/10.1021/es050400s.
Price, P.S., Jayjock, M.A., 2008. Available data on naphthalene exposures: strengths and limitations. Regul. Toxicol. Pharmcol. 51, 15–21. https://doi.org/10.1016/j.yrtph.2007.10.010.
Shao, M., Lu, S.H., Liu, Y., Xie, X., Chang, C.C., Huang, S., Chen, Z.M., 2009. Volatile organic compounds measured in summer in Beijing and their role in ground-level ozone formation. J. Geophys. Res. Atmos. 114, D00G06. https://doi.org/10.1029/2008JD010863.
Song, Y., Shao, M., Liu, Y., Lu, S.H., Kuster, W., Goldan, P., Xie, S.D., 2007. Source apportionment of ambient volatile organic compounds in Beijing. Environ. Sci. Technol. 41, 4348–4353. https://doi.org/10.1021/es0625982.
Tang, T.G., Cheng, Z.N., Xu, B.Q., Zhang, B.L., Zhu, S.Y., Cheng, H.R., Li, J., Chen, Y.J., Zhang, G., 2020. Triple isotopes ($\delta^{13}C$, $\delta^{2}H$, and $\Delta^{14}C$) compositions and source apportionment of atmospheric naphthalene: a key surrogate of intermediate-volatility organic compounds (IVOCs). Environ. Sci. Technol. 54, 5409–5418. https://doi.org/10.1021/acs.est.0c00075.
Uria-Tellaetxe, I., Navazo, M., de Blas, M., Durana, N., Alonso, L., Iza, J., 2016. Gas-phase naphthalene concentration data recovery in ambient air and its relevance as a tracer of sources of volatile organic compounds. Atmos. Environ. 131, 279–288. https://doi.org/10.1016/j.atmosenv.2016.01.047.
Wang, B.L., Liu, Y., Shao, M., Lu, S.H., Wang, M., Yuan, B., Gong, Z.H., He, L.Y., Zeng, L. M., Hu, M., Zhang, Y.H., 2016. The contributions of biomass burning to primary and secondary organics: a case study in Pearl River Delta (PRD), China. Sci. Total Environ. 569–570, 548–556. https://doi.org/10.1016/j.scitotenv.2016.06.153.
Wang, C.M., Wu, C.H., Wang, S.H., Qi, J.P., Wang, B.L., Wang, Z.L., Hu, W.W., Chen, W., Ye, C.S., Wang, W.J., Sun, Y.L., Wang, C., Huang, S., Song, W., Wang, X.M., Yang, S. X., Zhang, S.Y., Xu, W.Y., Ma, N., Zhang, Z.Y., Jiang, B., Su, H., Cheng, Y.F., Wang, X. M., Shao, M., Yuan, B., 2020. Measurements of higher alkanes using NO+PTR-ToF-MS: significant contributions of higher alkanes to secondary organic aerosols in China. Atmos. Chem. Phys. Discuss. https://doi.org/10.5194/acp-2020-145.
Wang, H.L., Chen, C.H., Wang, Q., Huang, C., Su, L.Y., Huang, H.Y., Lou, S.R., Zhou, M., Li, L., Qiao, L.P., Wang, Y.H., 2013. Chemical loss of volatile organic compounds and its impact on the source analysis through a two-year continuous measurement. Atmos. Environ. 80, 488–498. https://doi.org/10.1016/j.atmosenv.2013.08.040.
Watson, J.G., Chow, J.C., Fujita, E.M., 2001. Review of volatile organic compound source apportionment by chemical mass balance. Atmos. Environ. 35, 1567–1584. https://doi.org/10.1016/S1352-2310(00)00461-1.
Wu, L.Q., Wang, X.M., Lu, S.H., Shao, M., Ling, Z.H., 2019. Emission inventory of semi-volatile and intermediate-volatility organic compounds and their effects on secondary organic aerosol over the Pearl River Delta region. Atmos. Chem. Phys. 19, 8141–8161. https://doi.org/10.5194/acp-19-8141-2019.
Wu, H., Lu, L.P., Chen, J.Y., Zhang, C.L., Liu, W.P., Zhuang, S.L., 2020. Inhibited nitric oxide production of human endothelial nitric oxide synthase by nitrated and oxygenated polycyclic aromatic hydrocarbons. Environ. Sci. Technol. 54, 2922–2930. https://doi.org/10.1021/acs.est.9b07163.
Wu, R.R., Xie, S.D., 2018. Spatial distribution of secondary organic aerosol formation potential in China derived from speciated anthropogenic volatile organic compound emissions. Environ. Sci. Technol. 52, 8146–8156. https://doi.org/10.1021/acs.est.8b01269.
Yang, W.Q., Zhang, Y.L., Wang, X.M., Li, S., Zhu, M., Yu, Q.Q., Li, G.H., Huang, Z.H., Zhang, H.N., Wu, Z.F., Song, W., Tan, J.H., Shao, M., 2018. Volatile organic compounds at a rural site in Beijing: influence of temporary emission control and wintertime heating. Atmos. Chem. Phys. 18, 12663–12682. https://doi.org/10.5194/acp-18-12663-2018.
Xie, M., Barsanti, K.C., Hannigan, M.P., Dutton, S.J., Vedal, S., 2013. Positive matrix factorization of PM2.5-eliminating the effects of gas/particle partitioning of semivolatile organic compounds. Atmos. Chem. Phys. 13, 7381–7393. https://doi.org/10.5194/acp-13-7381-2013.
Yang, Y.Y., Guo, P.R., Zhang, Q., Li, D.L., Zhao, L., Mu, D.H., 2010. Seasonal variation, sources and gas/particle partitioning of polycyclic aromatic hydrocarbons in Guangzhou, China. Sci. Total Environ. 408, 2492–2500. https://doi.org/10.1016/j.scitotenv.2010.02.043.
Yuan, B., Shao, M., de Gouw, J., Parrish, D.D., Lu, S.H., Wang, M., Zeng, L.M., Zhang, Q., Song, Y., Zhang, J.B., Hu, M., 2012. Volatile organic compounds (VOCs) in urban air: how chemistry affects the interpretation of positive matrix factorization (PMF) analysis. J. Geophys. Res. Atmos. 117, D24302. https://doi.org/10.1029/2012JD018236.
Yuan, B., Hu, W.W., Shao, M., Wang, M., Chen, W.T., Lu, S.H., Zeng, L.M., Hu, M., 2013. VOC emissions, evolutions and contributions to SOA formation at a receptor site in eastern China. Atmos. Chem. Phys. 13, 8815–8832. https://doi.org/10.5194/acp-13-8815-2013.
Yuan, H.S., Tao, S., Li, B.G., Lang, C., Cao, J., Raymond, M.C., 2008. Emission and outflow of polycyclic aromatic hydrocarbons from wildfires in China. https://doi.org/10.1016/j.atmosenv.2008.05.033, 42, 6828-6835.

Yu, Q.Q., Gao, B., Li, G.H., Zhang, Y.L., He, Q.F., Deng, W., Huang, Z.H., Ding, X., Hu, Q. H., Huang, Z.Z., Wang, Y.J., Bi, X.H., Wang, X.M., 2016. Attributing risk burden of $PM_{2.5}$-bound polycyclic aromatic hydrocarbons to major emission sources: case study in Guangzhou, South China. Atmos. Environ. 142, 313–323. https://doi.org/10.1016/j. atmosenv.2016.08.009.

Zhao, Y.L., Hennigan, C.J., May, A.A., Tkacik, D.S., de Gouw, J.A., Gilman, J.B., Kuster, W.C., Borbon, A., Robinson, A.L., 2014. Intermediate-volatility organic compounds: a large source of secondary organic aerosol. Environ. Sci. Technol. 48, 13743–13750. https://doi.org/10.1021/es5035188.

Zhao, Y.L., Nguyen, N., Presto, A.A., Hennigan, C.J., May, A.A., Robinson, A.L., 2015. Intermediate volatility organic compound emissions from on-road diesel vehicles: chemical composition, emission factors, and estimated secondary organic aerosol production. Environ. Sci. Technol. 49, 11516–11526. https://doi.org/10.1021/acs.est.5b02841.

Zhao, Y.L., Nguyen, N., Presto, A.A., Hennigan, C.J., May, A.A., Robinson, A.L., 2016. Intermediate volatility organic compound emissions from on-road gasoline vehicles and small off-road gasoline engines. Environ. Sci. Technol. 50, 4554–4563. https://doi.org/10.1021/acs.est.5b06247.

Zhang, Y.L., Wang, X.M., Barletta, B., Simpson, I.J., Blake, D.R., Fu, X.X., Zhang, Z., He, Q.F., Liu, T.Y., Zhao, X.Y., 2013. Source attributions of hazardous aromatic hydrocarbons in urban, suburban and rural areas in the Pearl River Delta (PRD) region. http://doi.org/10.1016/j.jhazmat.2013.02.023, 250–251, 403-411.

Zhang, Y.L., Yang, W.Q., Simpson, I., Huang, X.Y., Yu, J.Z., Huang, Z.H., Wang, Z.Y., Zhang, Z., Liu, D., Huang, Z.Z., Wang, Y.J., Pei, C.L., Shao, M., Blake, D.R., Zheng, J. Y., Huang, Z.J., Wang, X.M., 2018. Decadal changes in emissions of volatile organic compounds (VOCs) from on-road vehicles with intensified automobile pollution control: case study in a busy urban tunnel in south China. Environ. Pollut. 233, 806–819. https://doi.org/10.1016/j.envpol.2017.10.133.

Zhang, Y.S., Shao, M., Lin, Y., Luan, S.J., Mao, N., Chen, W.T., Wang, M., 2013. Emission inventory of carbonaceous pollutants from biomass burning in the Pearl River Delta Region, China. Atmos. Environ. Times 76, 189–199. https://doi.org/10.1016/j.atmosenv.2012.05.055.

Zhang, Y.X., Tao, S., 2009. Global atmospheric emission inventory of polycyclic aromatic hydrocarbons (PAHs) for 2004. Atmos. Environ. 43, 812–819. https://doi.org/10.1016/j.atmosenv.2008.10.050.

Zhang, Z., Zhang, Y.L., Wang, X.M., Lv, S.J., Huang, Z.H., Huang, X.Y., Yang, W.Q., Wang, Y.S., Zhang, Q., 2016. Spatiotemporal patterns and source implications of aromatic hydrocarbons at six rural sites across China's developed coastal regions. J. Geophys. Res. Atmos. 121, 6669–6687. https://doi.org/10.1002/2016JD025115.